UNIVERSITÀ DEL PIEMONTE ORIENTALE

SCHOOL OF MEDICINE

Department of Health Sciences

Master's Degree in Medical Biotechnologies

Human Cytomegalovirus Infection Drives Cellular Senescence in Human Endothelial Cells

Tutor:

Professor. Marco De Andrea

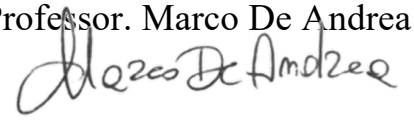

Candidate:

Dalia Sultan

Matricula Number:
20058769

Co-tutor:

Stefano Angelo Garagnani, PhD Student

Academic Year
2025/2026

Table of Contents

ABSTRACT *4*

Background: **4**

Objective: **4**

Methods: **4**

Results: **4**

Conclusion: **5**

INTRODUCTION *6*

Cellular senescence **6**

Historical perspective and definition 6

Senescence hallmarks: 6

Triggers of senescence 10

Virus induced senescence **12**

Human cytomegalovirus (HCMV) **13**

Epidemiology and clinical significance 13

Chronic Productive Infection 15

Latent Infection 15

Molecular Triggers of Reactivation 16

Virion structure of Human Cytomegalovirus 16

Envelope Glycoproteins and Their Functions 16

Composition and Function of Tegument 16

THE MAIN OBJECTIVE *19*

MATERIALS AND METHODS *20*

1.Cells culture and viruses **20**

2. Plaque Assay **20**

3.Western Blot Analysis **20**

4.Immunofluorescence Microscopy **21**

5.EdU Proliferation Assay **21**

6.Propidium Iodide Permeability Assay **21**

7.Multiplex immunoassay of cytokines/chemokines **22**

8.Transcriptomic Analysis **22**

9.RNA Extraction and Library Construction **23**

10.Comet Assay **23**

11.Immunofluorescence Analysis of CCFs and DNA Damage after STING Inhibition 23

12.Sting inhibition assay and cytokine quantification using ELISA.....24

RESULTS*.....*24

1. HCMV efficiently infects and fully replicates in HUVECs.....24

2. Endothelial cells exhibit signature of vascular disease and inflammation.....27

3. HCMV-infected HUVECs are susceptible to senescence processes 28

4.Senescence-associated gene expression in HCMV-infected HUVECs 29

5.HCMV-infected HUVECs have a diminished capacity to enter the S phase of the cell cycle 30

6.HCMV infection results in reduced levels of Lamin B1 and increased levels of $p16^{INK4A}$ in HUVECs 31

7.HCMV infection induces paracrine overexpression of NF-κB.....32

8.HCMV infection causes DNA damage and cytoplasmic chromatin fragments in HUVECs 33

9.STING antagonist suppresses cytokine release in HCMV-infected HUVECs 34

10.HCMV is responsible for creating cytoplasmic chromatin fragments in HUVECs.....35

CONCLUSION*.....*36

BIBLIOGRAPHY:* *37

ABSTRACT

Background:

Vascular disease and age-related inflammatory disorders have been epidemiologically associated with human cytomegalovirus (HCMV), a ubiquitous β-herpesvirus that establishes lifetime persistence in the host. Cellular senescence is characterized by irreversible cell-cycle arrest and a pro-inflammatory senescence- associated secretory phenotype (SASP), and it contributes to aging and age-related diseases. HCMV infects endothelial cells—key components of the vascular system—and modulates host cell-cycle regulation; however, whether HCMV actively induces a full senescence program in endothelial cells and the molecular mechanisms involved remain poorly defined.

Objective:

This study aims to determine whether HCMV infection induces cellular senescence in human umbilical vein endothelial cells (HUVECs) and to investigate the molecular pathways underlying this response.

Methods:

HUVECs were infected with the HCMV TR strain (MOI 3). Viral replication was assessed by western blotting, immunofluorescence, and plaque assay. Senescence was evaluated using EdU proliferation assays, western blotting for senescence-associated markers, and immunofluorescence detection for p16 ^{INK4a} , γH2AX, and NF-κB. DNA damage was measured by comet assay and by quantifying cytoplasmic chromatin fragments (CCFs). The involvement of the cGAS-STING pathway's involvement was teste using the STING inhibitor H-151. Secretion of cytokines secretion (IL-6, IL-8, IFN-β) was assessed by ELISA.

Results:

HUVECs supported productive HCMV replication. Infected cells displayed hallmarks of senescence, including reduced proliferation, Lamin B1 downregulation, p16 INK4a upregulation, and increased SASP secretion (IL-6, IL-8, CCL5). NF-κB nuclear translocation extended to bystander cells, indicating consistent with paracrine inflammatory signaling. HCMV infection also induced DNA damage and promoted the formation of CCFs.

Conclusion:

These findings support that HCMV infection induces cellular senescence in primary human endothelial cells, providing a mechanistic link between HCMV and vascular aging through virus-induced senescence (VIS).

INTRODUCTION

Cellular senescence

Historical perspective and definition

Cellular senescence is a state of stable and irreversible cell cycle arrest that occurs in response to various forms of cellular stress. It, a major discovery by Hayflick and Moorhead (1961), is a mechanism that universally regulates cell destiny and can be observed as a marker of aging[1,2]. Cellular senescence is a sustained arrest of the cell cycle that is distinguished by significant phenotypic alterations. It was initially identified in research on human fibroblasts that stopped proliferating after prolonged culture. It exerts negative impacts by inhibiting tissue repair and regeneration, contributing to tissue and organismal aging by the increase of senescent cells, depletion of stem/progenitor cell compartments, and the release of the senescence-associated secretory phenotype (SASP)[3].

Senescent cells maintain metabolic activity yet stop proliferating and frequently display phenotypic alterations, including enlarged morphology, and the release of pro-inflammatory factors collectively referred to as the senescence-associated secretory phenotype (SASP)[4].

Cells can undergo senescence due to a multitude of intrinsic and extrinsic factors, such as progressive telomere shortening, changes in telomeric structure, mitogenic signals, oncogenic activation, radiation, oxidative and genotoxic stress, epigenetic changes, chromatin disorganization, mitochondrial dysfunction, inflammation, and/or tissue damage signals, irradiation, or chemotherapeutic agents, nutrient deprivation[5–10].

Senescence hallmarks:

A common feature of senescent cells is a mostly irreversible cell-cycle arrest, potentially functioning as an alarm response activated by deleterious stimuli or aberrant growth. In mammalian cells, the retinoblastoma family (RB) and p53 proteins are important in arresting the senescent cell cycle[11]. RB1 and its family members p107 (RBL1) and p130 (RBL2) are phosphorylated by specific cyclin-dependent kinases. This phosphorylation reduces the ability of RB family members to repress the activity of the E2F family transcription factor, which is required for cell cycle progression[12]. However, in senescent cells, the CDK2 inhibitor $p21^{WAF1/Cip1}$ (CDKN1A) and the CDK4/6 inhibitor $p16^{Ink4a}$ (CDKN2A) accumulate. This accumulation leads to persistent activation of RB family proteins, inhibition of E2F transactivation and a resulting cell cycle arrest that cannot be reversed over time by subsequent inactivation of RB family proteins or p53[13].

In the p53/ $p21^{CIP1}$ pathway, phosphorylation activates p53 (p-p53) following a DNA-damaging event, which subsequently promotes the temporary expression of the cyclin-dependent kinase inhibitor $p21^{CIP1}$. $p21^{CIP1}$ then acts to inhibit CDK2-cyclin E, facilitating the dephosphorylation of RB, which results in the sequestration of E2F, thereby arresting the cell cycle.

The p53/ $p21^{CIP1}$ pathway is implicated in several types of senescence, including replicative senescence, DNA damage response (DDR)-induced senescence, Reactive Oxygen Species (ROS)-induced senescence, and oncogene-induced senescence (OIS), and is believed to be activated early in the senescence process. Conversely, the $p16^{Ink4a}$ /RB pathway is typically activated during replicative senescence, ROS-induced senescence, and OIS, but is not activated in DDR-induced senescence, and it is thought to have a more significant role in sustaining the senescent state[13,14].

Telomere length reflects cells' proliferative ability, which changes over time. It was shown that telomeres in highly proliferative somatic tissues, such as human fibroblasts, leukocytes, and adipocytes were shorter than in cells of non- or low rate proliferative tissues[15].

The most popular biomarker for identifying senescent cells, particularly those arising from replicative exhaustion, remains the detection of increased lysosomal β-galactosidase activity, termed senescence-associated β-galactosidase (SA-β-gal)[16,17].This assay capitalizes on a distinct biochemical property: while lysosomal β-galactosidase activity in normal, young cells is optimal at an acidic pH of 4, a specific isoform or modification of the enzyme in senescent cells exhibits detectable activity at a less acidic pH of 6. This activity is typically visualized histochemically using the chromogenic substrate 5-bromo-4-chloro-3-indolyl β-D-galacto-pyranoside (X-Gal) at pH 6.0[17–19]. The correlation between increasing SA-β-gal activity and in vitro aging has been demonstrated across multiple cell types and species. Notably, studies have shown that SA-β-gal-positive cell counts increase as a function of population doubling level (PDL), often in parallel with telomere shortening a main driver of replicative senescence [20].

Despite its widespread use, the specificity and mechanistic role of SA-β-gal as a senescence marker are subjects of ongoing scrutiny. Genetically disrupting lysosomal β-galactosidase does not prevent cells from entering senescence, indicating that the enzyme is not a direct trigger of the senescent program but rather a frequent companion to it[21,22]. Therefore, while a robust and convenient histological marker, SA-β-gal positivity should be

interpreted as a common correlation of the senescent state rather than its definitive cause, and its findings are best supported by additional senescence hallmarks.

Biochemically, β-galactosidase is a lysosomal hydrolase that cleaves terminal β-d-galactose residues from substrates such as glycoproteins, glycolipids, and glycosaminoglycans. At high concentrations, it can contribute to extracellular matrix remodeling through the hydrolysis of glycosidic bonds in proteoglycans. Deficiencies in this enzyme are linked to lysosomal storage disorders, including galactosialidosis and Morquio B syndrome. The enzyme itself is regulated post-translationally; its 86-kDa precursor form is processed to a mature 64-kDa enzyme by lysosomal proteases, with cathepsins playing a key role in its maturation, while other proteases mediate its eventual degradation[23].

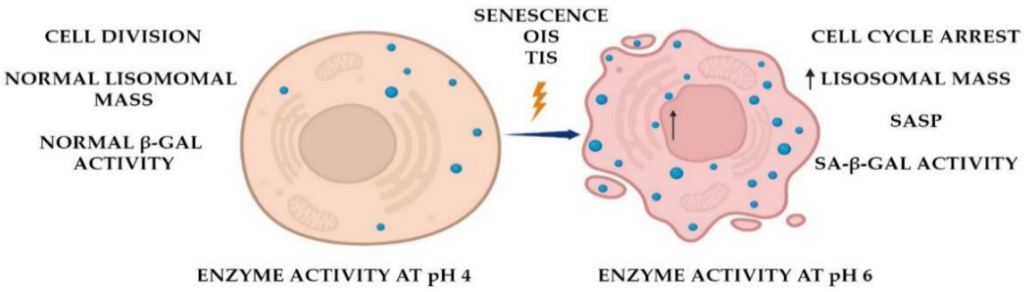

Figure1: Biological role of senescence-associated β-galactosidase[24].

In addition to previously described markers, cellular senescence is also characterized by structural alterations and degradation of the nuclear lamina. The nuclear lamina is a filamentous net lining the inner nuclear membrane, essential for maintaining nuclear shape, mechanical stability, and size[25,26]. Its primary structural constituents are the nuclear lamins, type V intermediate filament proteins of 60–80 kDa, categorized into A-type (lamin A, C) and B-type (lamin B1, B2) based on biochemical properties[27]. This structure is highly dynamic, undergoing complete disassembly during mitosis and reassembly thereafter to accommodate cell division[28,29].

A-type lamins, lamin A and its splice variant lamin C, are encoded by the *LMNA* gene and are upregulated during cellular differentiation[30]. While lamin A is dispensable for cell growth in certain contexts—mice expressing only lamin C develop normally—mutations in *LMNA* that produce aberrantly processed or misfolded lamin A proteins underlie a spectrum of human diseases known as laminopathies[31]. These include muscular dystrophy, cardiomyopathy, lipodystrophy, and Hutchinson–Gilford progeria syndrome (HGPS). HGPS is specifically

caused by the accumulation of a truncated, permanently farnesylated lamin A variant called progerin, which induces accelerated cellular senescence[32]. Notably, low-level progerin expression has also been detected during physiological aging, suggesting a potential link between lamin A dysfunction and normal aging processes[33].

In contrast, B-type lamins (lamin B1 and B2) are encoded by separate genes (*LMNB1*, *LMNB2*) and are expressed in most cell types throughout development. Although certain cell types, such as embryonic stem cells, can proliferate in the absence of lamins, lamin B1 is crucial for proper organogenesis and postnatal survival Lmnb1 null mice die shortly after birth[34], and their fibroblasts exhibit nuclear dysmorphology and premature senescence. While A- and B-type lamins form distinct but interconnected filament networks, they functionally interact[35].

The cyclic GMP-AMP synthase–stimulator of interferon genes (cGAS–STING) signaling axis constitutes a fundamental cytosolic DNA-sensing mechanism essential for innate antiviral immunity [36,37]. Upon engagement with double-stranded DNA, typically of microbial origin, cGAS catalyzes the synthesis of the cyclic dinucleotide second messenger 2'3'-cGAMP. This molecule binds and activates the endoplasmic reticulum adaptor protein STING, initiating a downstream signaling cascade. Activated STING recruits and facilitates the autophosphorylation of TANK-binding kinase 1 (TBK1), which in turn phosphorylates the transcription factor interferon regulatory factor 3 (IRF3) and activates nuclear factor-kappa B (NF-κB). The subsequent nuclear translocation of IRF3 and NF-κB drives the transcriptional upregulation of type I interferons and pro-inflammatory cytokines, establishing a potent host defense response against intracellular pathogens[36,38,39].

Beyond its canonical role in pathogen sensing, emerging evidence has established the cGAS-STING pathway as a critical regulator of sterile inflammation, particularly in the context of cellular senescence. It is now recognized that self-derived nuclear DNA fragments can aberrantly accumulate in the cytoplasm of senescent cells, where they act as endogenous ligands for cGAS, thereby activating the SASP. The sources of this immunostimulatory DNA are multifaceted and linked to hallmark senescent alterations[40,41]:

1. **Cytoplasmic chromatin fragments (CCFs)**, which arise from nuclear envelope destabilization frequently associated with lamin B1 downregulation.
2. **Mitochondrial DNA (mtDNA)** is released due to organellar dysfunction.
3. **Micronuclei and nuclear buds** containing missegregated chromosomes.
4. **Retrotransposon-derived cDNA**.

Under homeostatic conditions, such aberrant cytosolic DNA is swiftly degraded by dedicated nucleases, including three-prime repair exonuclease 1 (TREX1) and deoxyribonuclease II (DNase II), to prevent inadvertent activation of innate immune sensors. However, in senescence, the expression of these safeguard enzymes is often suppressed a process potentially mediated by the repression of E2F transcription factors, which are common transcriptional targets during cell cycle arrest. The resulting failure of cytosolic DNA clearance permits persistent cGAS-STING activation[42]. This sustained signaling, predominantly through the NF-κB branch, acts as a direct transcriptional driver for the expression of core SASP components, such as interleukin-6 (IL-6) and chemokine (C-X-C motif) ligand 8 (CXCL8/IL-8). Consequently, the cGAS-STING pathway serves as a pivotal molecular transducer, converting the intracellular biomarker of genomic stress persistent cytosolic DNA into the chronic, pro-inflammatory secretory phenotype that defines the senescent state and mediates its pathophysiological effects.

Triggers of senescence

Cellular senescence can be triggered by a variety of intrinsic and extrinsic stressors, among them we can describe:

- Replicative senescence→ This refers to the decrease in proliferative capacity that occurs after many cell divisions, eventually leading to total arrest[1]. This type of senescence is attributed to the shortening of telomeres caused by many cell divisions in non-transformed cells[12].

DNA damage-induced senescence→ Depending on the severity of the damage, irreversible DNA damage might result in senescence or apoptosis. In vitro, many DNA-damaging agents are utilized to induce this type of senescence, including radiation (ionizing and UV) and numerous medicines[43]. DNA damage agents and telomere loss stimulate the DNA-damage response (DDR), which directly activates p53 and p21, its downstream transcriptional target.

Oncogene-induced senescence (OIS)→ the activation of oncogenes like (Ras or BRAF) or the inactivation of tumor suppressors can lead to OIS[12,44] and this activates p16 and p53 with the DDR and ARF.
Mitochondrial dysfunction-associated senescence→ It was recently shown that inducing mitochondrial malfunction causes senescence. The phenotype, especially the SASP, appears to be typical of this kind of senescence[44].
Senescence-associated secretory phenotype→ Senescent cells exhibit a complex pro-inflammatory response termed the senescence-associated secretory phenotype (SASP)[45].

This phenotype is regulated by the transcription factors nuclear factor-κB (NF-κB) and CCAAT/enhancer-binding protein-β (CEBPβ), leading to the secretion of pro-inflammatory cytokines (interleukin-6 and 8), chemokines (monocyte chemoattractant proteins (MCPs) and macrophage inflammatory proteins (MIPs)), growth factors (transforming growth factor-β (TGFβ) and granulocyte–macrophage colony-stimulating factor (GM-CSF)), and proteases[46]. Notably, SASP components, particularly TGFβ, can induce senescence in neighboring cells via a paracrine mechanism that produces reactive oxygen species (ROS) and DNA damage[47].

Virus induced senescence

Viral infection activates multiple cellular stress response pathways, including heat shock, oxidative stress, and the DNA damage response (DDR), which may induce apoptosis or autophagy[48,49]. Typically, these cellular mechanisms help restrict viral replication. Nevertheless, certain viruses have evolved mechanisms to evade or manipulate these antiviral responses to facilitate their own replication.

The activation of stress response pathways by viruses can also result in the induction of cellular senescence. Recent studies have highlighted a significant and multifaceted intersection between virology and the biology of aging, focusing on the concept of virus-induced senescence (VIS).

An increasing amount of evidence suggests that viral infections can serve as a powerful trigger cellular senescence. Various types of viruses, including RNA viruses like SARS-CoV-2 and DNA viruses such as herpesviruses (for instance, human cytomegalovirus and Kaposi's sarcoma-associated herpesvirus), as well as hepatitis B virus and retroviruses like HTLV-1, have been found to trigger a senescent state in host.

Human cytomegalovirus (HCMV)

Epidemiology and clinical significance

HCMV is one of eight double-stranded DNA human herpesviruses known to induce chronic or latent disease in an infected host[50].

Human cytomegalovirus (HCMV) is a prototypical beta-herpesvirus that infects a majority of the world's population. Although most HCMV infections are asymptomatic in healthy individuals, the virus is the leading cause of congenital abnormalities following fetal infection and is a significant cause of morbidity and mortality following hematopoietic stem cell transplant and solid organ transplant[51,52]

Human cytomegalovirus (HCMV), a β-herpesvirus, is a highly prevalent virus infecting 40–100% of the population worldwide[53].It establishes a lifelong latent infection, with reactivations and reinfections sporadically[54]. Most of the early life CMV infections are asymptomatic due to effective immune response and are transmitted postnatally through saliva or breast milk following reactivation of the latent virus in the mother. Congenital CMV infection is rare but can cause symptomatic, even severe infection [55].

However, primary infection or viral reactivation can cause serious multiorgan disease in immunocompromised individuals. Various risk groups, such as transplant recipients, intensive care patients, acquired immunodeficiency syndrome (AIDS) patients, and fetuses/newborns, are susceptible to the development of HCMV-mediated disease due to the impaired immune response[56,57]. Several common risk factors associated with HCMV infection include being female, older age, low socioeconomic status, and weakened immunity[58,59]. HCMV is primarily transmitted through bodily fluids such as blood, urine, and saliva, with salivary and sexual contact being the main routes[60,61]. HCMV also poses serious risks to organ transplant recipients and individuals with acquired immunodeficiency syndrome (AIDS), whether it originates from primary infection or reactivation of a latent infection. Complications such as HCMV retinitis, pneumonia, and gastrointestinal disorders, including gastroenteritis, hepatitis, and colitis, are commonly observed in organ or bone marrow transplant recipients and immunocompromised individuals, particularly those with AIDS[62,63].

Human cytomegalovirus (HCMV) infection is linked to the induction of pro-inflammatory signaling pathways[64,65]. Principally, the virus activates the nuclear factor-kappa B (NF-κB) pathway, a controller of genes involved in inflammatory responses. This activation, which can be initiated via viral engagement of host pattern recognition receptors (PRRs) such as Toll-like receptors (TLRs), results in the production of inflammatory mediators. Among these, cytokines like interleukin-6 (IL-6) and tumor necrosis factor-alpha (TNF-α) are established as major contributors to inflammation. Ultimately, this cascade alters immune cell composition and functionality [66].

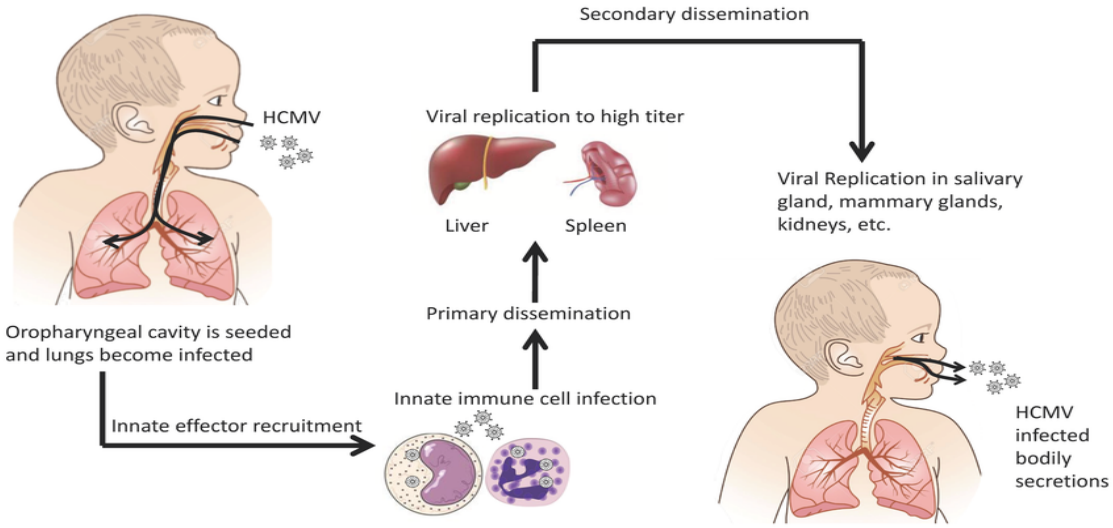

Figure2: Overview of human cytomegalovirus (HCMV) dissemination[60].

HCMV spread within the populous by several routes. Vertical transmission occurs through transplacental and intrapartum transmission through breast feeding from an infected mother to the child [67–70]. Horizontal transmission occurs by organ transplantation of an infected organ or contact with infected bodily secretions (i.e., saliva, breast milk, urine, etc.)[71–74].Post-exposure, human cytomegalovirus (HCMV) is understood to initiate a brief period of leukocyte-associated viremia, facilitating primary viral dissemination to and productive infection of organ systems including the lung, spleen, and liver[75]. This tropism for secretory epithelia is presumed to be an adaptive mechanism, aligning with the virus's reliance on bodily fluid contact for inter-host transmission.

The initiation of viral dissemination is contingent upon viral entry and replication within a permissive host cell following breaching of external barriers. Experimental evidence from murine cytomegalovirus (MCMV) indicates that alveolar macrophages and type II

pneumocytes constitute the initial cellular targets after intranasal inoculation[76], a model that can be extrapolated to hypothesize the primary infection sites for human cytomegalovirus (HCMV). Cellular entry of HCMV into epithelial lineages and macrophages is achieved through endocytic uptake and subsequent low-pH-triggered fusion with the endosomal membrane, facilitated by key viral glycoprotein complexes, notably gB, the trimer gH/gL/gO, and the pentamer gH/gL/UL128- 131A[77–81]. After entry, the virus executes its lytic replication cycle within the epithelial cell, producing infectious virions capable of infecting a diverse array of secondary cell types, such as fibroblasts, endothelial cells, dendritic cells, and other innate immune effectors like alveolar macrophages[82,83]. This early local dissemination is propagated via two distinct mechanisms: the release of cell-free viral particles and direct cell-to-cell spread[84]. Cell-to-cell transmission, which necessitates intimate cellular contact, is partially governed by the product of the HCMV gene US28[85].

Following primary infection, human cytomegalovirus (HCMV) establishes a life-long persistence within the host through two distinct but interconnected states: chronic productive infection and true latency. The specific contributions of each state to overall viral persistence are not fully understood.

Chronic Productive Infection

Chronic infection is characterized by the prolonged, low-level shedding of infectious virus from specific sites within the host. This state can originate from an unresolved primary infection or from the reactivation of latent virus and may serve to replenish latent reservoirs. In immunocompetent individuals, chronic shedding is typically asymptomatic, though it has been epidemiologically linked to inflammatory and age-related conditions, such as vascular disease[86–90],Key sites of chronic shedding include endothelial and epithelial cells. For instance, HCMV is frequently shed in breast milk during the postpartum period[70] and can be excreted in urine for extended periods in pediatric patients[89].

Latent Infection

In contrast, latent infection is defined by a reversibly quiescent state where the viral genome persists in host cells without producing infectious virions. Viral gene expression is severely restricted, with only a subset of latency-associated transcripts expressed. The potential for reactivation back to a productive lytic cycle is a defining feature that distinguishes true latency from an abortive infection. Reactivation can be triggered by several factors, including the loss of T-cell-mediated immune surveillance or changes in the cellular differentiation/activation state of the latently infected cell (e.g., monocytes differentiating

into macrophages). While sporadic reactivation events likely occur in healthy individuals, they are swiftly controlled by existing cellular immunity and do not cause disease. However, severe HCMV disease arises when reactivation and subsequent chronic replication proceed unchecked due to insufficient T-cell control, as seen in transplant recipients, individuals with HIV/AIDS, or patients undergoing intensive chemotherapy[89,91].

Molecular Triggers of Reactivation

The molecular switch from latency to reactivation is tightly coupled to host cell signaling. The major immediate-early promoter (MIEP), which controls the expression of key viral lytic genes, is densely populated with binding sites for host transcription factors such as NF-κB, AP-1, and CREB. Consequently, inflammatory signals, cellular stress, and differentiation cues that activate these pathways can efficiently trigger reactivation. Notably, HCMV infection itself can promote a pro-inflammatory state; for example, it alters the transcriptome of infected monocytes, biasing their differentiation toward pro-inflammatory M1 macrophages, a process that may inadvertently create a cellular environment permissive for viral reactivation[92].

Virion structure of Human Cytomegalovirus

The mature human cytomegalovirus (HCMV) virion exhibits a complex, multilayered architecture with 150–200 nm diameter[93]. Its core consists of a 100-nm icosahedral nucleocapsid housing the 230-kilobase pair (kbp), double-stranded linear DNA genome. This nucleocapsid is encased by a dense, proteinaceous layer termed the tegument or matrix. The outermost layer is a host-derived phospholipid envelope embedded with numerous virally encoded glycoproteins.

Envelope Glycoproteins and Their Functions

The viral envelope contains several essential glycoproteins, including gpUL55 (glycoprotein B, gB), gpUL73 (gN), gpUL74 (gO), gpUL75 (gH), UL100 (gM), and gpUL115 (gL). These surface proteins are critical for multiple stages of the viral life cycle, mediating initial attachment and fusion with host cell membranes, facilitating cell-to-cell spread, and contributing to virion assembly and maturation[94].

Composition and Function of Tegument

The tegument layer is composed of phosphorylated, highly immunogenic proteins that are delivered into the host cell upon viral entry. While involved in virion maturation, their primary significance lies in their ability to influence early post-entry events. These include facilitating

the release of the viral genome from the capsid and the immediate regulation of both viral and host gene promoters.

The most abundant tegument proteins are ppUL32 (pp150 or the basic phosphoprotein) and ppUL83 (pp65). Due to its high abundance, pp65 serves as the target antigen in antigenemia assays, which are used for the rapid diagnosis of active HCMV infections in clinical settings.

Importantly, the tegument contains key regulatory proteins that act as transcriptional transactivators, profoundly impacting host cell physiology.

ppUL69 stimulates expression from the viral major immediate-early enhancer-promoter (ie1/ie2). It is essential for efficient viral replication and induces cell cycle arrest in the G1 phase through unknown mechanism[95,96].

ppUL82 (pp71) functions as a transcriptional activator, stimulating the ie1/ie2 promoter via cellular transcription factors such as activating transcription factor/cyclic AMP-response element binding protein (ATF/CREB) and activator protein-1 (AP-1). It enhances the infectivity of viral DNA, is required for efficient replication at low multiplicities of infection and accelerates the G1 to S phase transition in quiescent cells[97–99].

Additional transactivator proteins, including pIRS1 and pTRS1, are also associated with virions [100].

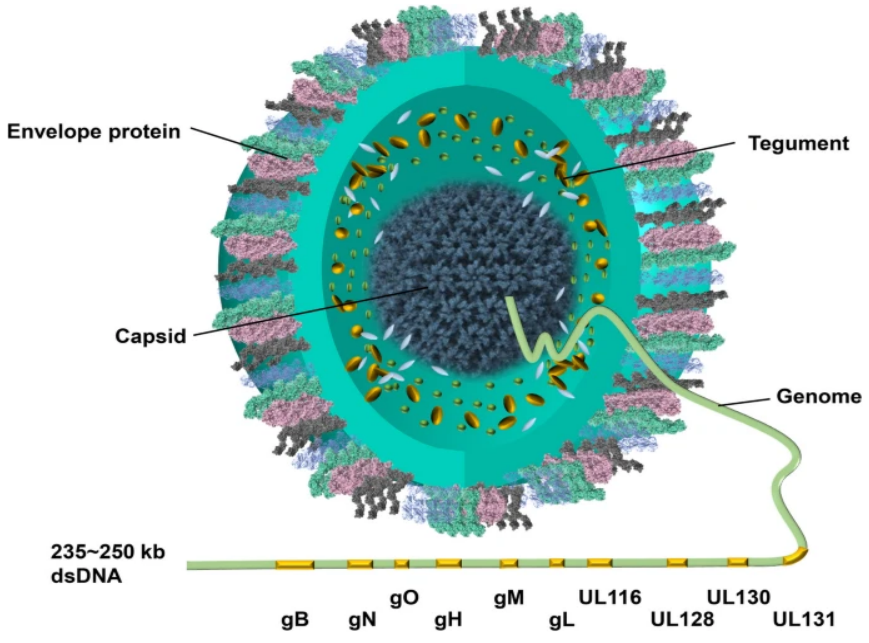

Figure3: Structure of the human cytomegalovirus (HCMV) virion and its components[101].

Our group has previously shown that a cellular senescence program, characterized by premature senescence mediated by p53 and p16INK4a, is triggered in primary human fibroblasts by Human Cytomegalovirus (HCMV) infection. HCMV infection of renal proximal tubular epithelial cells (RPTECs) causes a senescence-associated secretory phenotype (SASP) and, notably, an IL-6-dependent paracrine senescence loop that transmits senescence signals to nearby uninfected cells[102]. The paracrine amplification of senescence was only seen in epithelial cells of renal origin, proving that HCMV-induced senescence is not cell type specific, occurring in both fibroblasts and renal epithelial cells.

Endothelial cells play an important role in cardiovascular disease, atherosclerosis, and vascular problems associated with aging. Because HCMV is epidemiologically associated to vascular disease and accelerated aging, HUVECs are an important and physiologically useful model for studying virus-induced endothelium dysfunction and senescence.

THE MAIN OBJECTIVE

Previous findings from our group demonstrated that HCMV infection is able to induce cellular senescence in RPTECs, a well-established in vitro model of kidney epithelial cells. Considering that endothelial cells play a crucial role in vascular homeostasis and represent an important target of viral infection, it remains unclear whether this pro-senescent effect is cell type–specific or reflects a more general host response. HUVECs, widely used as a model of vascular endothelium, provide a suitable system to address this question. Therefore, the aim of this thesis is to investigate whether HCMV can induce cellular senescence in HUVECs and to dissect the molecular targets and mechanisms underlying its action. Elucidating these aspects will help to clarify the impact of HCMV infection on endothelial cell biology and its potential contribution to vascular dysfunction.

MATERIALS AND METHODS

1.Cells culture and viruses

Human Umbilical Vein Endothelial pooled Cells (HUVECs, FB60C12203 Lot. 488Z001) were grown in Endothelial Cell Growth Medium containing additional VEGF (EGM-2, PromoCell, Heidelberg, Germany). Human foreskin fibroblast (HFFs, ATCC SCRC-1041) and ARPE-19 cells (ATCC CRL-2302) were grown in high-glucose Dulbecco's modified Eagle's medium (DMEM, Sigma-Aldrich, Milan, Italy) supplemented with 10% fetal bovine serum (FBS, Sigma-Aldrich) and 1% penicillin streptomycin-gentamycin solution (Sigma-Aldrich). HCMV TR strain was propagated for one passage in HFFs and two passages in ARPE-19 cells using standard plaque assay. A standard plaque assay was performed on confluent HFFs to titrate the virus. For experiments, 9.0×10^4 (HUVEC cells) were seeded in 6 well plates and were infected at a multiplicity of infection (MOI) of 3. The infection was stopped after 24 hours by changing the media, then at 4-day post infection (dpi) and 7 dpi the media was added. Cells were observed and harvested at 2, 4, 6 and 8 dpi, considering the time of infection as day zero. The mock samples were the non-infected ones.

2. Plaque Assay

To determine viral titers ,2.5 × 104 HFFs were seeded in 96-well plates in DMEM supplemented with 10% FBS. The following day, ten-fold serial dilutions (from 10^{-1} to 10^{-7}) of either the HCMV TR strain stock or supernatants harvested from HCMV-infected HUVECs were prepared in culture medium. Each dilution was added to duplicate wells. A positive control (virus with a known titer) and a negative control (culture medium only) were included in each assay, centrifuged at 2000 rpm for 30 min, and incubated for 2 h at 37 °C. Supernatants were then discarded, and cells were layered with 0.8% methylcellulose for 8 days to allow plaque development. After 8 days, the methylcellulose layer was removed, and the cells were stained with 0.1% crystal violet, incubated at room temperature for 30 min on an orbital shaker, Excess stain was removed by gently washing the plates with tap water, and the plates were allowed to air dry. The plaques were manually counted under a microscope. Viral titers were calculated as plaque-forming units per milliliter (PFU/mL) using the following formula:

$$PFU/mL = \frac{Average\ number\ of\ plaques}{Dilution\ factor \times Volume\ of\ inoculum\ (mL)}$$

3.Western Blot Analysis

HUVECs were seeded in 6-well plates and infected with HCMV TR strain. Infected cells were collected at 2, 4, 6, and 8 days post-infection (dpi), with non-infected controls harvested at corresponding time points. Cells were lysed on ice using RIPA buffer (Pierce) supplemented with phosphatase (Thermo Fisher) and protease inhibitors (Sigma-Aldrich). Protein concentrations were quantified using Bradford reagent at 595 nm with a Nanophotometer.20 µg of protein extracts were separated on 7.5% and 12% SDS-PAGE gels (TGX™ FastCast™, Bio-Rad) and transferred

to nitrocellulose membranes (Trans-Blot® Turbo™, Bio-Rad). Membranes were blocked with 10% non-fat milk or BSA in TBST and incubated with primary antibodies overnight at 4°C, followed by HRP-conjugated secondary antibodies for 1 hour at room temperature. Bands were visualized using ECL substrate (Thermo Fisher) and the ChemiDoc™ MP Imaging System (Bio-Rad). Antibodies targeted: IEA, UL44, pp28, p53, $p16^{INK4a}$, $p21^{WAF1/Cip1}$, and Lamin B1. β-actin and vinculin served as loading controls.

4.Immunofluorescence Microscopy

HUVECs (1.9×10^4) were seeded in triplicate on coverslips in 24-well plates and infected with HCMV TR at MOI 3. At 4, 6, and 8 days post-infection (dpi), cells were Fixed with 4% paraformaldehyde for 15 minutes at RT then Permeabilized cells with 0.2% Triton-X100 for 20 minutes at 4°C. Blocked the cell membrane with PBS containing 1% BSA, 1% NGS, 0.05% Tween-20 for 15 minutes at RT.Incubate the cells with primary antibodies for 1 hour at RT in a humidified chamber. After this incubating with secondary antibodies (Alexa Fluor 488 anti-mouse, Alexa Fluor anti-rabbit) with 4',6-diamidino-2-phenylindole (DAPI) (D1306, Thermo Fischer Scientific, Waltham, MA, USA) to counterstain the nuclei for 1 hour at RT.Coverslips were mounted using SlowFade Gold and visualized with a Leica Thunder Imager 3D System.

Target proteins analyzed include IEA, UL44, pp28 (viral markers), NF-κB, p16INK4a, γH2AX (senescence markers). The percentage of positive cells was normalized to total DAPI-positive nuclei. Image analysis was performed using LAS X software, with values expressed as mean ± SD.

5.EdU Proliferation Assay

HUVECs (3.2×10^3) were seeded in triplicate in 96-well plates and cultured in EGM overnight. Cells were then infected with HCMV TR strain at an MOI of 3. Mock-infected cells served as controls.At 3, 5, and 7 dpi, cells were treated with 50 µM EdU for 20 hours to label proliferating cells. Following EdU incorporation, cells were Fixed with 4% paraformaldehyde (PAF) for 15 minutes at room temperature then Permeabilized with 1× saponin solution.Stained using the ClickTech EdU Cell Proliferation Kit 488 (baseclick GmbH) finally Counterstained with DAPI to visualize all nuclei. Images were acquired using a Cytation 5 Cell Imaging Multi-Mode Reader (Agilent BioTek) with a 10× objective . For each well, a 2 × 2 montage was captured in both fluorescent channels to visualize DAPI is for total nuclei (blue) and EdU is for Proliferating cells (green) then processed and stitched using the default setting of the proprietary software.

6.Propidium Iodide Permeability Assay

HUVECs (3.2×10^3 cells per well) were seeded in triplicate in 96-well plates and cultured in EGM overnight. Cells were then infected with HCMV TR strain at an MOI of 3. Mock-infected cells served as controls. At 4, 6, and 8 days dpi, the culture medium was removed, and cells were gently washed with PBS. Then, 100 µL of PBS containing Propidium Iodide was added to each well. Cells were incubated for 20 minutes at room temperature in the dark. Negative control is untreated (mock-infected) cells incubated with PI only and positive control is cells treated with PBS

containing 0.2% Triton X-100 to permeabilize the cell membrane completely. Fluorescence intensity was measured using a Spark multimode microplate reader (Tecan, Männedorf, Switzerland) at excitation/emission wavelengths appropriate for PI (typically ~535 nm/617 nm). Results were expressed as relative fluorescence units (RFU), with the positive control (Triton X-100-treated cells) representing 100% permeability.

7.Multiplex immunoassay of cytokines/chemokines

Supernatants collected from HCMV-infected and mock-infected HUVECs were analyzed for the presence of 27 human cytokines and chemokines using the Bio-Plex Pro™ Human Cytokine Grp I Panel 27-Plex kit (Bio-Rad Laboratories) .The assay was performed according to the manufacturer's instructions using the Bio-Plex 200 System (Bio-Rad Laboratories).

8.Transcriptomic Analysis

Total RNA was extracted from HCMV-infected and non-infected HUVECs using the miRNeasy Tissue/Cells Advanced Kit (Qiagen, Hilden, Germany). RNA quality was determined with the Agilent 4200 TapeStation system, and all samples had an RNA Integrity Number (RIN) greater than 8, suggesting high-quality RNA appropriate for sequencing. The Illumina TruSeq Stranded mRNA kit (Illumina, Inc., San Diego, CA, USA) was used to prepare libraries from 500 ng of total RNA per sample. mRNA sequencing was performed on an Illumina NextSeq550 sequencer (Illumina, Inc.) with the NextSeq 500/550 High Output Kit v2.5, 150 cycles and paired-end 2 × 75 bp reads. For each condition, two biological replicates were used, including infected and mock-infected samples.

The raw sequencing reads were processed using a bioinformatics pipeline. The STAR program was used to align reads to the reference human genome (hg38). Ensembl v100 annotations were set as the reference for the RSEM computational pipeline, which was employed to quantify gene expression levels. Differentially expressed genes (DEGs) were calculated using DESeq2 with thresholds of log2 fold change (log2FC) greater than 2 and an adjusted p-value (p.adj) less than 0.05 to determine statistical significance. All statistical and graphical computations were performed in the R environment (https://www.r-project.org/). Unsupervised hierarchical clustering of genes was visualized as a heatmap using the "heatmap" package in R, with expression values presented as log2-transformed.

Gene Set Enrichment Analysis (GSEA) was employed to investigate the cellular response to HCMV infection. GSEA was performed using the desktop application, and significantly enriched gene sets were filtered using the following cut-offs: a normalized enrichment score (|NES|) greater than 1 and a false discovery rate (FDR) q-value less than 0.05. This analysis allowed the identification of key biological pathways and processes modulated by HCMV infection in HUVECs.

9.RNA Extraction and Library Construction

For transcriptome analysis, total RNA was extracted from HCMV-infected and mock-infected HUVECs using the miRNeasy Tissue/Cells Advanced Kit (Qiagen, Hilden, Germany) according to the manufacturer's instructions. RNA quality was assessed using the Agilent 4200 TapeStation system with the HS D1000 RNA kit (Agilent, Santa Clara, CA, USA) . All samples exhibited an RNA Integrity Number (RIN) greater than 8, confirming the high quality and integrity of the extracted RNA for downstream sequencing applications.Library preparation was performed using the Illumina TruSeq Stranded mRNA kit (Illumina, Inc., San Diego, CA, USA) with 500 ng of total RNA per sample. The procedure included poly-A selection, fragmentation, reverse transcription, and adapter ligation according to the manufacturer's protocol. mRNA sequencing was conducted on an Illumina NextSeq 550 platform using the NextSeq 500/550 High Output Kit v2.5 (150 cycles, paired-end 2 × 75 bp read length). Two biological replicates were analyzed for each experimental condition.

10.Comet Assay

Slides were pre-coated with 1% normal melting agarose (NMA) and air-dried overnight.At the proper time points, 1×10^5 HUVECs were collected, resuspended in cold PBS, and stored on ice.Cells were mixed with 1% Low Melting Agarose (LMA) at 37°C, pipetted onto coated slides, covered with a coverslip, and allowed to solidify at 4°C for 10 minutes.The coverslips were removed, and the slides were submerged in ice-cold Complete Lysis Buffer (2.5 M NaCl, 100 mM EDTA, 10 mM Tris, 1% Triton X-100, pH 10.5) for 1 hour at 4°C.Slides were placed in an electrophoresis tray and coated with alkaline electrophoresis buffer (300 mM NaOH, 1 mM EDTA, pH >13) for 30 minutes at 4°C to allow DNA unwinding. Electrophoresis was carried out at 21 V, 400 mA for 30 minutes at 4°C. Slides were washed with neutralization buffer (0.4 M Tris-HCl, pH 7.5) for 15 minutes before staining with Propidium Iodide (10 µg/mL) for 20 minutes in the dark.A fluorescent microscope was used to obtain images at 10× and 20× magnification. The CometScore software was used to examine at least 50 cells from each sample. DNA damage was measured using the tail moment formula (tail length ×% DNA in tail). The results were reported as the mean tail moment ± SD.

11.Immunofluorescence Analysis of CCFs

HUVECs (1.9×10^4) were seeded in triplicate on coverslips in 24-well plates and treated with the STING inhibitor H-151 (4 µM) for 1 hour prior to infection with HCMV TR strain (MOI 3) or mock infection.Four experimental groups were included: mock, HCMV, mock + H-151, and HCMV + H-151.Next day,Stop the infection by changing the media.At 4 day post-infection (dpi), cells were Fixed with 4% paraformaldehyde for 15 minutes at RT then Permeabilized cells with 0.2% Triton-X100 for 20 minutes at 4°C. Blocked the cell membrane with PBS containing 1% BSA, 1% NGS, 0.05% Tween-20 for 15 minutes at RT.Incubate the cells with primary antibodies for 1 hour at RT in a humidified chamber. After this incubating with secondary antibodies (Alexa Fluor 488 anti-mouse, Alexa Fluor anti-rabbit) with 4',6-diamidino-2-phenylindole (DAPI) (D1306, Thermo Fischer Scientific, Waltham, MA, USA) to counterstain the nuclei for 1 hour at RT.Coverslips were mounted using SlowFade Gold and visualized with a Leica Thunder Imager 3D System.

12.Sting inhibition assay and cytokine quantification using ELISA

HUVECs were pre-treated with the STING inhibitor H-151 (4 μM) for 1 hour prior to infection with HCMV TR strain (MOI 3) or mock infection. Four experimental groups were included: mock, HCMV, mock + H-151, and HCMV + H-151. Next day, Stop the infection by changing the media. Supernatants were collected at 1, 2, and 3 days post-infection (dpi) , centrifuged, and stored at -80°C until analysis. Sandwich ELISA (R&D Systems DuoSet Kits) was used to quantify IL-6, IL-8, and IFN-β levels in supernatants, following product instructions. Briefly, 96-well plates were coated with capture antibody overnight, blocked, and then incubated with standards and samples. Following washing, a biotinylated detection antibody was applied, followed by Streptavidin-HRP. TMB substrate was added, reaction was halted with 2N H_2SO_4, and absorbance was measured at 450 nm. Cytokine concentrations were determined using the standard curve and reported as pg/mL (mean ± SD).

RESULTS

1. HCMV efficiently infects and fully replicates in HUVECs

To investigate endothelial cell susceptibility to HCMV infection, human umbilical vein endothelial cells (HUVECs) were exposed to the HCMV TR strain at a multiplicity of infection (MOI) of 3. Western blot analysis was used to analyze the kinetics of viral protein expression during different stages of

the viral life cycle. As shown in Figure 4A, the immediate-early protein IEA (IE1 and IE2) was detected at 2 days post-infection (dpi), followed by the early protein UL44 at 4 dpi and the late protein pp28 at 6 dpi.

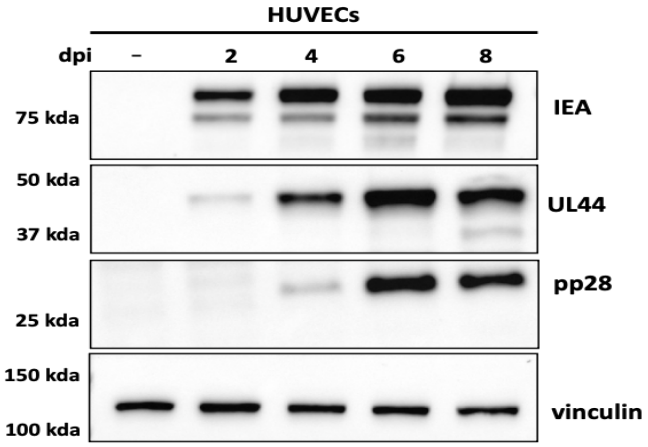

Figure4A:

Expression of HCMV viral proteins on HUVECs Kinetic of viral protein expression. Protein lysates from HUVECs infected at MOI 3 and harvested at different days post infection were subjected to immunoblotting using antibodies recognizing immediate early (IEA: IE1 and IE2), early (UL44), or late (pp28) viral antigens or with anti-Vinculin to show equal loading.

To investigate if HUVECs enhance productive viral replication, viral particles released into culture supernatants at 4, 6, and 8 days post infection using the standard plaque test were measured. Figure 4B shows that virus titers gradually grew to 1.5×10^4 PFU/mL by 8 days post-infection. Immunofluorescence analysis verified the infection's spread, with IEA-positive cells increasing from 25% at 2 dpi to 33% at 8 dpi (Fig. 4C). Overall, these data show that HUVECs are totally permissive to HCMV infection and promote the development of infectious viral progeny.

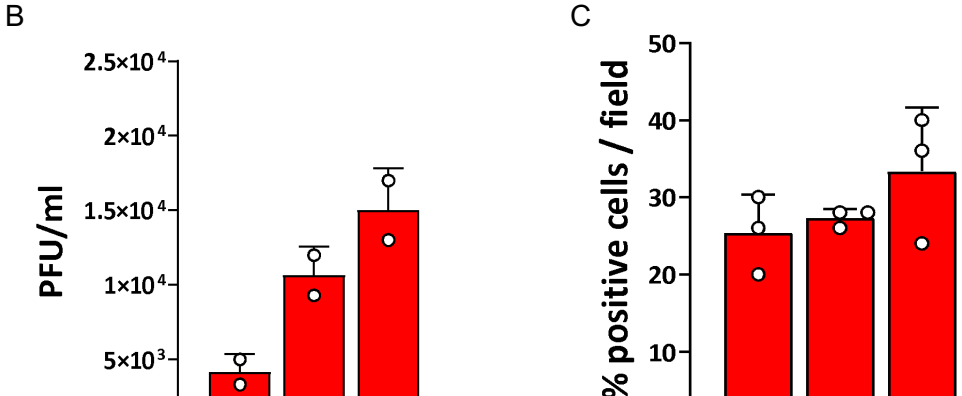

Figure 4:

B. The production of viral particles in HUVECs infected with HCMV TR at MOI 3 was measured by plaque assay on HFFs. At 4, 6 and 8 dpi, viral plaques were microscopically counted and expressed as PFU/mL B. Immunofluorescence analysis for viral protein IEA detection. Cells were infected as in Fig.3 and at different dpi immunofluorescence assay was performed. Cells were co-stained with antibodies anti-IEA and DAPI to detect nuclei. The histogram shows the percentage of IEA-positive cells per well at each time point. The percentage of cells expressing viral genes represent the mean of three replicated experiments. Values were expressed as mean ± SD (error bars).

2. Endothelial cells exhibit signature of vascular disease and inflammation

To identify the molecular changes caused by human cytomegalovirus (HCMV) in endothelial cells, transcriptome analysis of mock and HCMV-infected human umbilical vein endothelial cells (HUVECs) was performed on day 4 post-infection (dpi). The DisGeNET tool was used to evaluate the results of the RNA sequencing analysis and to identify gene signatures related to disease phenotypes. The results of the analysis showed that infected HUVECs have highly enriched gene signatures of vascular diseases and inflammatory responses. Figure 5 shows that the most enriched disease classes in infected cells are vascular diseases and inflammation. This suggests the possible involvement of HCMV in endothelial dysfunction.

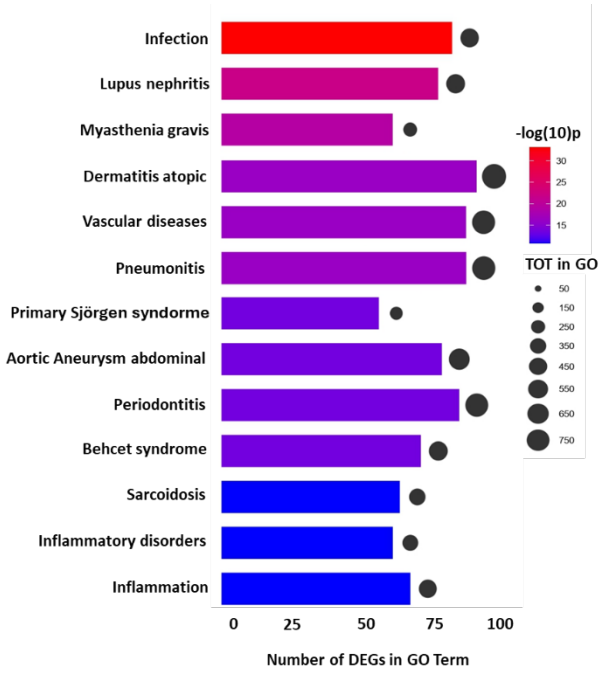

Figure 5: Transcriptome profile of HCMV-infected HUVECs based on DISGENET

Bar plot showing selective over-expression DisGeNET in HUVECs transcriptome upon HCMV infection (MOI 3). The y-axis indicates enriched diseases (including Vascular disease, Inflammation); the x-axis shows the number of differentially expressed genes (DEGs) in each respective disease. Circle size reflects the total number of genes in each respective disease, while color intensity (from red to blue) indicates statistically significance (red=higher significance).

3. HCMV-infected HUVECs are susceptible to senescence processes

To better understand the biological processes affected by HCMV infection, the transcriptome results were analyzed through the Metascape database. The results of the Gene Ontology (GO) analysis showed significant upregulation of genes involved in “positive regulation of cytokine production” and “negative regulation of cell population proliferation” (Fig. 6). This led to an investigation of whether HCMV-infected endothelial cells are susceptible to senescence.

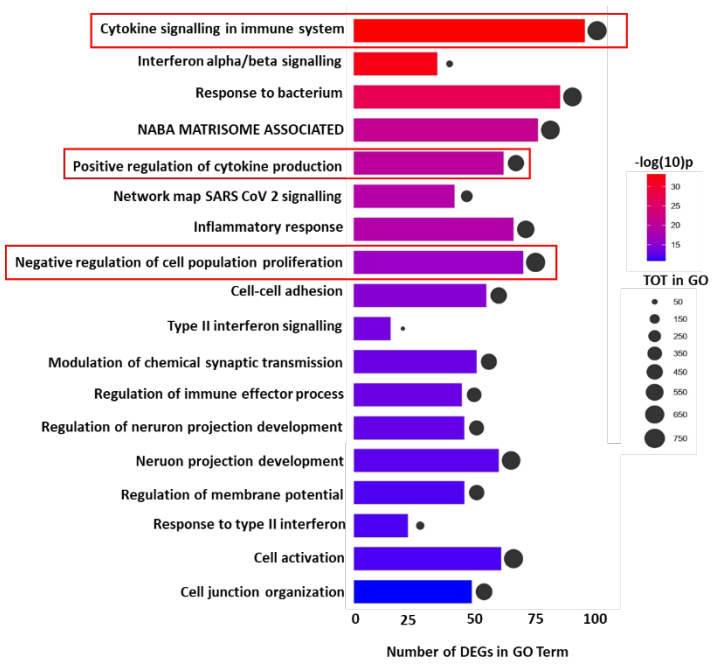

Figure 6: Transcriptional response to HCMV infection in HUVECs

Bar plot showing selective over-expression Gene Ontology (GO) Term in HUVECs transcriptome upon HCMV infection (MOI 3). The y-axis indicates enriched biological processes (including Positive regulation of cytokine production, Negative regulation of cell population proliferation); the x-axis shows the number of differentially expressed genes (DEGs) in each respective GO Term. Circle size reflects the total number of genes in each respective GO Term, while colour intensity (from red to blue) indicates statistically significance (red=higher significance).

4.Senescence-associated gene expression in HCMV-infected HUVECs

Following the transcriptome analysis, the current investigation sought to assess whether it is possible to identify a signature of senescence in human umbilical vein endothelial cells (HUVECs) infected with cytomegalovirus (HCMV). To achieve this, the SenMayo gene set, a novel and validated method for the identification of senescent cells in different tissues and cells, was used. Using the Gene Set Enrichment Analysis (GSEA), it was evident that there existed an enriched signature of senescence and SASP-related genes in HCMV-infected cells compared to mock-infected cells (nominal p-value = 0.008; Fig. 7).

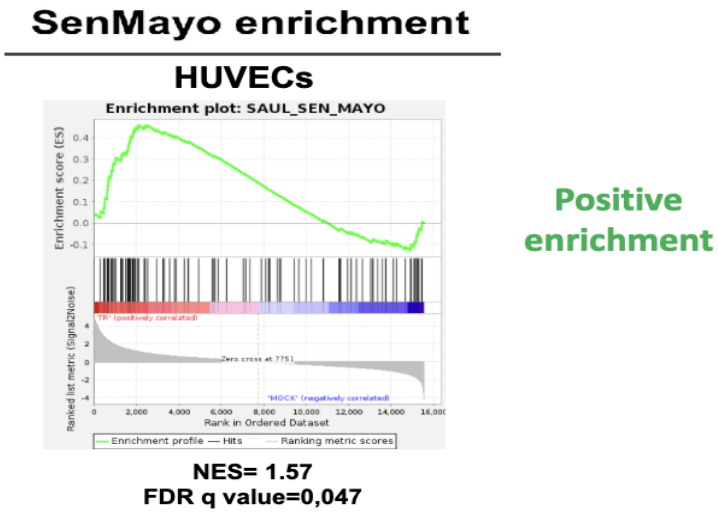

Figure 7: GSEA of the comparison between HCMV-infected and mock-infected HUVECs, showing the enrichment of senescence genes associated with the SenMayo signature. Gene Set Enrichment Analysis (GSEA) of the comparison between HCMV-infected and mock-infected cells, showing the enrichment of senescence genes associated with the SenMayo signature in HUVECs. The enrichment score curve is depicted in green, with genes on the far left (red) correlating with HCMV-infected cells, and genes on the far right (blue) correlating with mock-infected cells. The vertical black lines indicate the position of each gene in the gene set analyses. Normalized enrichment score (NES) and Nominal p value are shown.

5.HCMV-infected HUVECs have a diminished capacity to enter the S phase of the cell cycle

To functionally validate the predicted senescence phenotype, the proliferative capacity of HCMV-infected HUVECs was examined by assessing the proportion of cells that incorporated the nucleotide analog 5-ethynyl-2'-deoxyuridine (EdU) into newly synthesized DNA. As shown in Figure 8B, the proportion of cells positive for EdU incorporation was significantly lower in HCMV-infected HUVECs than in mock-infected cells at all examined time points. The proportion of cells positive for EdU incorporation decreased from 23.89% to 12.32% at 4 dpi, from 16.51% to 4.31% at 6 dpi, and eventually to 0.38% at 8 dpi in HCMV-infected HUVECs compared to 12.63% at 8 dpi in mock-infected cells.

To ensure that the diminished capacity of HCMV-infected HUVECs to incorporate EdU into their DNA was not because of increased rates of cell death, we performed a Propidium Iodide (PI) permeability assay to assess the viability of cells at each time point. As shown in Figure 8C, no statistically significant difference in PI permeability was observed between HCMV-infected HUVECs and mock-infected cells at any time point.

A

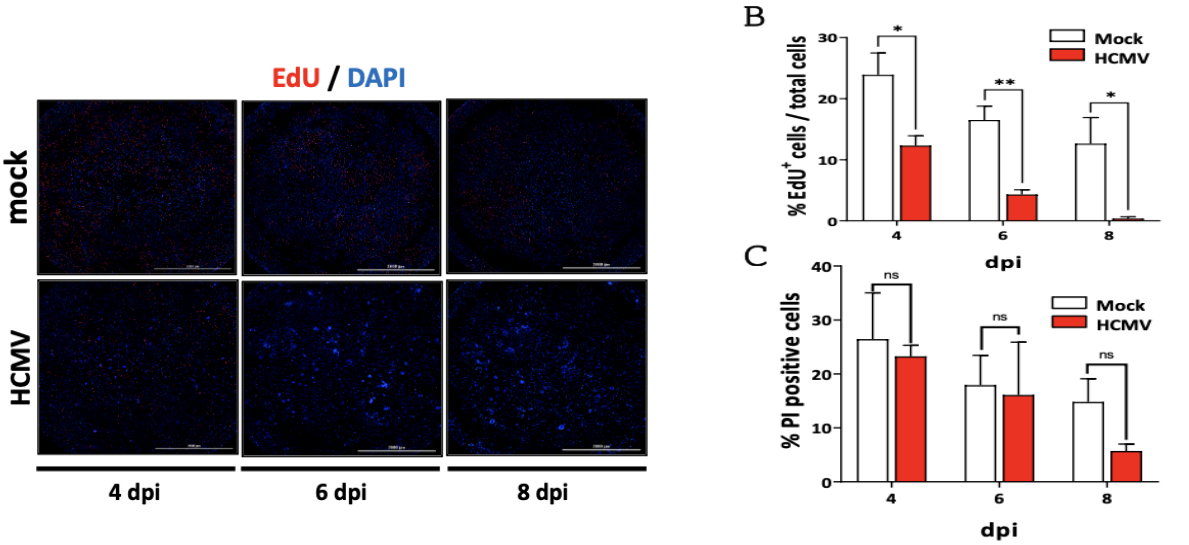

Figure 8: HCMV-induced decrease in HUVECs proliferation

A. Representative EdU staining of mock and infected HUVECs at 4, 6 and 8 dpi. Cells were infected at MOI 3 and subjected to EdU for 16 h. Nuclei were counterstained with DAPI. Red signals indicate Edu positive cells. B. This histogram shows the percentage of EdU positive cells and the total number of cells. There is a significant decrease of EdU positive cells between mock and infected HUVECs. C. At 4, 6 and 8 dpi mock and infected HUVECs at MOI 3 were incubated with Propidium Iodide for 20 minutes. This graph shows the percentage of Propidium Iodide positive cells that are not statistically significant between mock and infected HUVECs. Values were expressed as mean ± SD (error bars).

6.HCMV infection results in reduced levels of Lamin B1 and increased levels of p16^{INK4A} in HUVECs

Since senescence is characterized by multiple markers rather than single markers, we investigated the expression levels of some established markers of senescence. Western blot analysis revealed that the levels of Lamin B1 progressively reduced during HCMV infection of HUVECs. At the same time, there was an upregulation of p16^{INK4A}, suggesting that cell cycle arrest might be mediated by this pathway. However, no significant change was observed in the levels of p53 and p21$^{WAF1/Cip1}$ (Fig. 9).

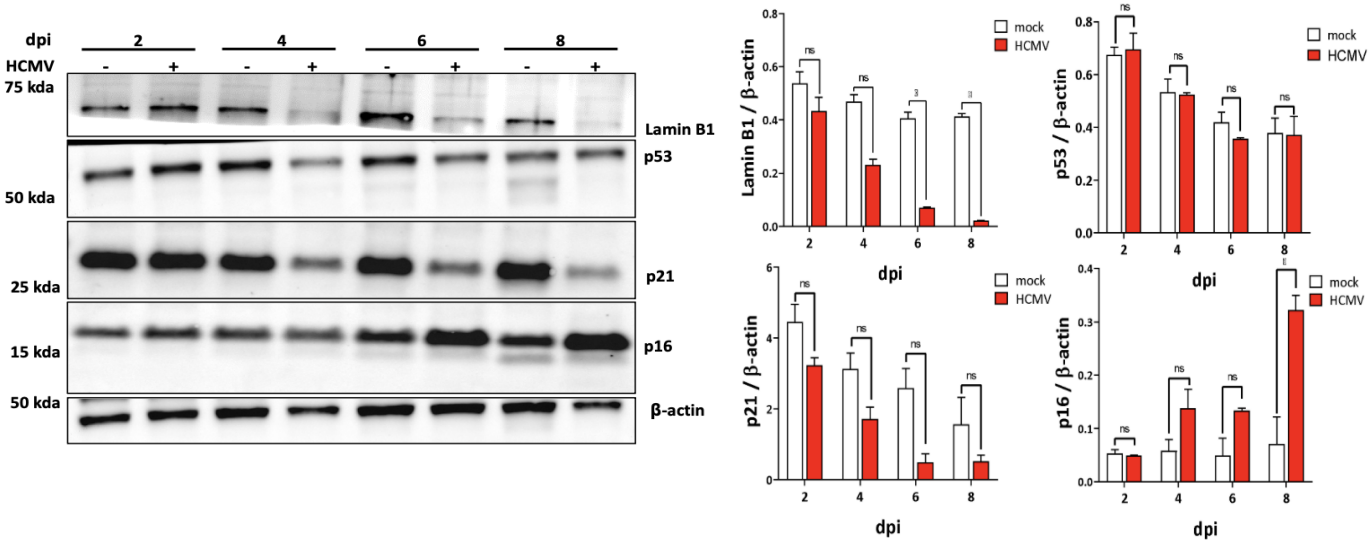

Figure 9: Senescence markers expression in HUVECs

Western Blot analysis shows the senescence markers expression in HUVECs infected with HCMV TR at MOI 3. Lysates were probed with antibodies against the indicated targets; β-actin is used as protein loading control. In densitometric analysis band intensities were quantified using Image Lab (Bio-Rad) and a statistical analysis was performed with GraphPad Prism. Values were expressed as mean ± SD (errors bars).

7.HCMV infection induces paracrine overexpression of NF-κB

To better define the senescence-like phenotype and assess its paracrine characteristics, co-immunofluorescence assays were performed to detect the HCMV immediate early antigen protein along with established markers of senescence, $p16^{INK4A}$, γH2AX, and NF-κB. As expected from the results shown in Figure 12, $p16^{INK4A}$ and γH2AX were found to be highly expressed within IEA+ cells at all time points examined, confirming that these are HCMV-specific events within the infected cells. Interestingly, the translocation of NF-κB, a hallmark of inflammatory pathway activation, was also detected within the neighboring non-infected cells.

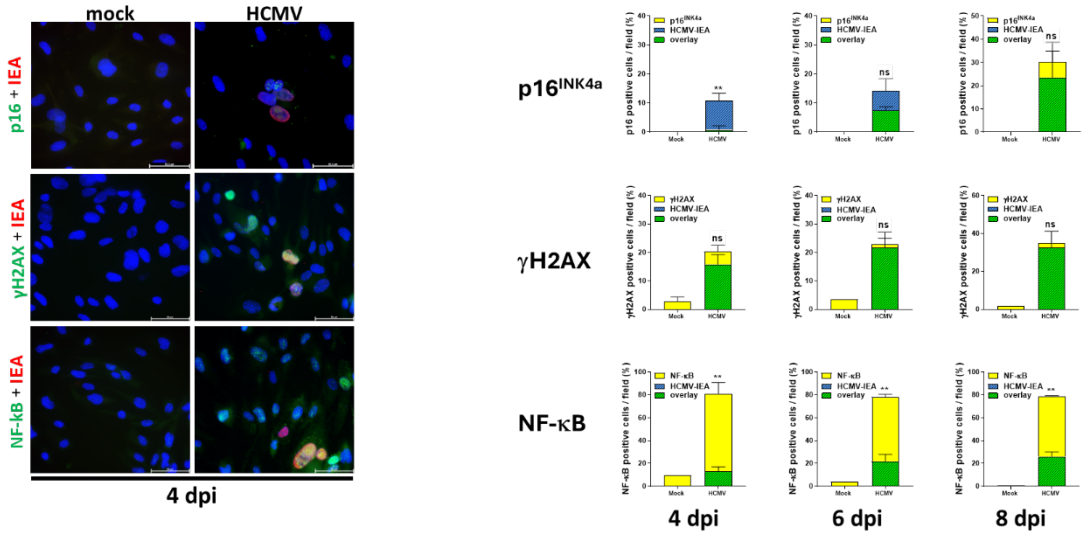

Figure 10: Paracrine inflammation in HUVECs upon HCMV infection

Representative immunofluorescence images at the indicated time points showing co-staining of $p^{16INK4A}$, γH2AX and NF-κB in green with HCM Immediate Early Antigen (IEA). Cells were infected with MOI3 and were analyzed at 4, 6 and 8 dpi. Nuclei were counterstained with DAPI (blue). The panel shows the quantification of p16INK4A/γH2AX/NF-κB positive nuclei and IEA-positive cells per field. Values were expressed as mean ± SD (errors bars).

8.HCMV infection causes DNA damage and cytoplasmic chromatin fragments in HUVECs

To assess whether HCMV infection causes genotoxic stress in HUVECs, the comet assay was performed. This technique detects double strand breaks by assessing the migration of fragmented DNA outside of the nucleus, which creates a distinctive comet tail shape.
Immunofluorescence analysis of HCMV-infected cells revealed the formation of cytosolic DNA, which were evident as DAPI-positive structures outside the nucleus 4 days post-infection. The comet tails of HCMV infected HUVECs were significantly longer than those of mock infected controls specially at 4 dpi (Figure 12A). The tail moment (a composite of tail length and percentage of DNA in comets) was significantly elevated for the infected cells compared to the mock cells. The tail moments reached 10 for the infected cells at 4 dpi, while those of the mock cells had slight differences ($p < 0.01$, Figure 12B).

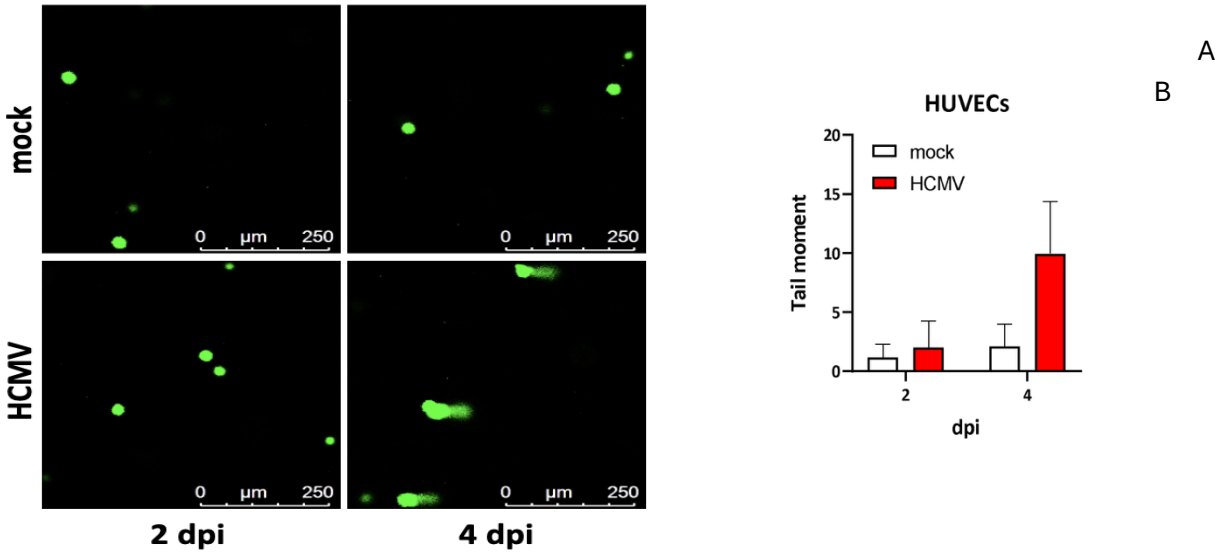

Figure12:

HCMV induces DNA damage in HUVECs assessed by comet assay. HUVECs were infected with HCMV TR strain at MOI 3, and DNA damage was evaluated at 2 and 4 dpi using the alkaline comet assay. ***(A)*** *Representative immunofluorescence images intact DNA remains in the nucleus (head), while fragmented DNA migrates to form a tail.* ***(B)*** *Quantification of DNA damage expressed as tail moment (tail length × percentage of DNA in tail). Values were expressed as mean ± SD (errors bars).*

9.STING antagonist suppresses cytokine release in HCMV-infected HUVECs

To further investigate the role of the cGAS-STING pathway in HCMV-induced inflammatory cytokine release, HUVECs were treated with the STING inhibitor H-151 (4 μM) before infection with HCMV. The culture medium was collected at 1, 2, and 3 dpi, and the cytokine levels of IL-6, IL-8, and IFN-β were measured using an ELISA assay. As shown in Figure 13 Regarding IL-6, All mock infected had a baseline of about 100 pg/ml. HCMV infected displayed a progressive increase in IL-6 secretion ranging from 200 pg/ml on day 1 to up to 2000 pg/ml on day 3. Treatment with H-151 significantly suppressed this response lowering IL-6 secretion too near baseline (100-200 pg/ml). For IL-8, HCMV infection caused a very strong induction of IL-8 release that reached up to 9000 pg/ml on day 3. However, mock infected cells did not increase and remained at 100 pg/ml. Treatment with H-151 significantly reduced IL-8 concentrations from HCMV infection. Regarding IFN-β, HCMV infection induced a marked increase in the levels of IFN-β by day 3. However, mock infected cells had IFN-β at baseline levels. The use of H-151 to inhibit STING completely abolished the production of IFN-β to near baseline levels. Taken together these data suggest that activation of STING is required for the pro-inflammatory response in endothelial cells infected with HCMV. H-151 (4 μM) treatment resulted in complete abolishment of IL-6 and IL-8 but not IFN-β secretion and would suggest that the cGAS-STING pathway is responsible for driving the SASP (senescence associated secretory phenotype) in HCMV infected HUVEC. This result also indicates the occurrence of other pathway able to induce the release of IFN-β, such as RIG-I or the TLR receptors.

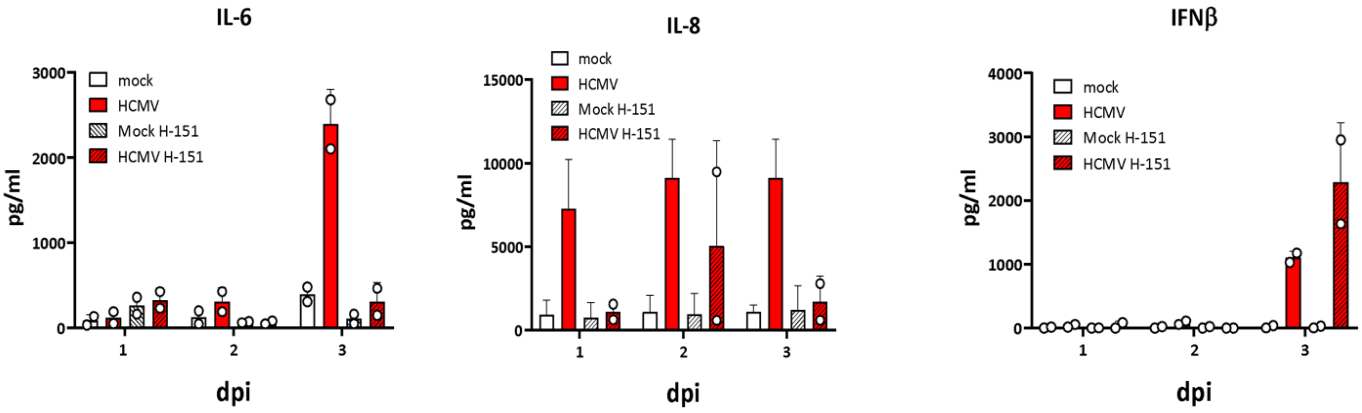

Figure13:

Impact of STING inhibition on cytokine secretion in HCMV-infected HUVECs at MOI 3. Supernatants were collected after 1, 2, and 3 dpi, and IL-6, IL-8, and IFN-β secretion was quantified using ELISAs. Four experimental groups were included: mock-infected, HCMV-infected, HCMV-infected with H-151 treatment, and mock-infected with H-151 treatment alone. Values were expressed as mean ± SD (errors bars).

10.HCMV is responsible for creating cytoplasmic chromatin fragments in HUVECs

Following the observation of DNA damage by Comet assay, we investigated whether HCMV infection induces CCF formation in HUVECs. To achieve this, immunofluorescence assays were carried out at 4 dpi with HCMV. DAPI was used as a DNA-binding fluorescent probe, γH2AX as a DNA damage marker, and IEA as a viral infection marker.

As shown in Figure 14, in HCMV-infected cells, cytoplasmic DAPI staining was observed as foci of chromatin fragments (CCFs), indicated by arrows. These chromatin fragments in the cytoplasm of HCMV-infected cells were associated with γH2AX staining, indicating DNA damage response in the cells. The merged figure further confirms the presence of chromatin fragments in the cytoplasm of HCMV-infected cells (IEA staining), indicating this is a direct result of viral infection. The finding of CCFs in HCMV-infected HUVECs has important implications, since these cytoplasmic DNA fragments can activate the cGAS-STING pathway leading to the activation of IRF3 and NF-κB with subsequent production of IFN-β and proinflammatory cytokines (IL-6 and IL-8).The results from the Comet assay and the formation of CCFs upon HCMV infection in HUVECs have provided a mechanistic explanation for the DNA damage caused by HCMV and the efflux of chromatin fragments from the nuclei into the cytoplasm.

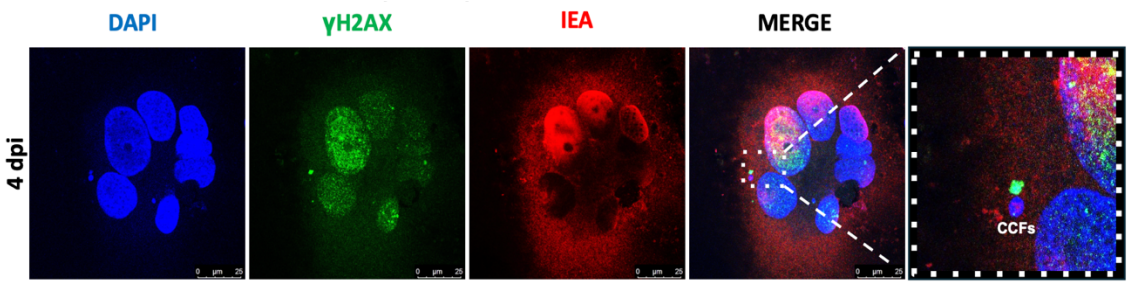

Figure 14:

HCMV induces CCFs formation in HUVECs. Immunofluorescence images of HCMV-infected HUVECs at 4 dpi showing DAPI (nuclei and CCFs), γH2AX (DNA damage), IEA (viral infection), and merge. White arrows indicate CCFs (DAPI-positive foci in the cytoplasm).

CONCLUSION

Cellular senescence is a state of stable and irreversible cell cycle arrest contributing to general physical decline and age-related disease. it can be caused by a variety of intrinsic and extrinsic factors, including viral infections, which have lately emerged as powerful inducers via a phenomenon known as virus-induced senescence (VIS).

In this study, we provide comprehensive evidence that human cytomegalovirus (HCMV) can efficiently infect and replicate in primary human umbilical vein endothelial cells (HUVECs),This is shown by the expression of viral proteins from different phases of the viral replication cycle, namely, immediate-early (IEA), early (UL44), and late (pp28) phases, and the production of infectious viral progeny. Approximately 30% of cells are productively infected, and titers rise to 1.5×10^4 PFU/mL by eight days post-infection. This shows that HUVECs can be a robust model in vitro for studying the interaction between HCMV and endothelial cells.

Transcriptome profiling of human umbilical vein endothelial cells (HUVECs) infected with human cytomegalovirus (HCMV) has shown enrichment of gene signatures related to vascular diseases and inflammatory responses, this suggests a possible role of HCMV in the pathogenetic mechanisms of vascular disorders. In addition, analysis of Gene Ontology found that there was upregulation of the genes associated with "positive regulation of cytokine production" and "negative regulation of cell population proliferation", raising important questions about whether HCMV induces cellular senescence. By utilizing the validated SenMayo gene set, Functional validation confirmed that HCMV infection significantly reduces the ability of cells to proliferate evidenced by the marked drop in EdU incorporation in HCMV infected cells.

In the study, HCMV-infected HUVECs displayed a strong senescence phenotype with less Lamin B1 levels, more $p16^{INK4a}$ levels, and a different profile of SASP factors (e.g., IL-6, IL-8, CCL5). Using immunofluorescence, $p16^{INK4a}$and γH2AX protein expression were only present in HCMV infected cells, while the nuclear translocation of NF-κB could be seen in both HCMV-infected and adjacent, uninfected cells, this indicates the presence of paracrine inflammatory signals emanating from the infected HUVECs.

HCMV infection caused DNA damage, as demonstrated by increased comet tail moment and the development of cytoplasmic chromatin fragments (CCFs) 4 days after infection. STING was inhibited with the specific antagonist H-151 (4 μM) resulting in a total block of IL-6 and IL-8 secretion levels while there was still persistence of γH2AX foci indicating that DNA damage happens upstream of STING activation, whereas CCF formation and the senescence-associated secretory phenotype (SASP) seems to be STING dependent.

These results show that there is a direct link between HCMV infection and endothelial senescence through a pathway that involves DNA damage, CCF formation, and STING-mediated inflammatory signaling, providing a rationale for the epidemiological association between HCMV infection and vascular disease.

BIBLIOGRAPHY:

1. Hayflick, L. & Moorhead, P. S. The serial cultivation of human diploid cell strains. *Experimental cell research* **25**, 585–621 (1961).

2. López-Otín, C., Blasco, M. A., Partridge, L., Serrano, M. & Kroemer, G. The hallmarks of aging. *Cell* **153**, 1194–1217 (2013).

3. Campisi, J., Andersen, J. K., Kapahi, P. & Melov, S. Cellular senescence: a link between cancer and age-related degenerative disease? in vol. 21 354–359 (Elsevier, 2011).

4. Coppé, J.-P. *et al.* Senescence-associated secretory phenotypes reveal cell-nonautonomous functions of oncogenic RAS and the p53 tumor suppressor. *PLoS biology* **6**, e301 (2008).

5. Di Micco, R. *et al.* Interplay between oncogene-induced DNA damage response and heterochromatin in senescence and cancer. *Nature cell biology* **13**, 292–302 (2011).

6. Kuilman, T., Michaloglou, C., Mooi, W. J. & Peeper, D. S. The essence of senescence. *Genes & development* **24**, 2463–2479 (2010).

7. Passos, J. F. *et al.* Feedback between p21 and reactive oxygen production is necessary for cell senescence. *Molecular systems biology* **6**, 347 (2010).

8. Pazolli, E. *et al.* Chromatin remodeling underlies the senescence-associated secretory phenotype of tumor stromal fibroblasts that supports cancer progression. *Cancer research* **72**, 2251–2261 (2012).

9. García-Prat, L. *et al.* Autophagy maintains stemness by preventing senescence. *Nature* **529**, 37–42 (2016).

10. Mikuła-Pietrasik, J., Niklas, A., Uruski, P., Tykarski, A. & Książek, K. Mechanisms and significance of therapy-induced and spontaneous senescence of cancer cells. *Cellular and Molecular Life Sciences* **77**, 213–229 (2020).

11. Rodier, F. & Campisi, J. Four faces of cellular senescence. *Journal of Cell Biology* **192**, 547–556 (2011).

12. Sharpless, N. E. & Sherr, C. J. Forging a signature of in vivo senescence. *Nature Reviews Cancer* **15**, 397–408 (2015).

13. Beauséjour, C. M. *et al.* Reversal of human cellular senescence: roles of the p53 and p16 pathways. *The EMBO journal* (2003).

14. Dulić, V., Beney, G.-E., Frebourg, G., Drullinger, L. F. & Stein, G. H. Uncoupling between phenotypic senescence and cell cycle arrest in aging p21-deficient fibroblasts. *Molecular and cellular biology* **20**, 6741–6754 (2000).

15. Daniali, L. *et al.* Telomeres shorten at equivalent rates in somatic tissues of adults. *Nature communications* **4**, 1597 (2013).

16. Gary, R. K. & Kindell, S. M. Quantitative assay of senescence-associated β-galactosidase activity in mammalian cell extracts. *Analytical biochemistry* **343**, 329–334 (2005).

17. Dimri, G. P. *et al.* A biomarker that identifies senescent human cells in culture and in aging skin in vivo. *Proceedings of the National Academy of Sciences* **92**, 9363–9367 (1995).

18. Pati, S. *et al.* X-gal staining of canine skin tissues: a technique with multiple possible applications. *Journal of Natural Science, Biology, and Medicine* **5**, 245 (2014).

19. Kurz, D. J., Decary, S., Hong, Y. & Erusalimsky, J. D. Senescence-associated β-galactosidase reflects an increase in lysosomal mass during replicative ageing of human endothelial cells. *Journal of cell science* **113**, 3613–3622 (2000).

20. Matsunaga, H. *et al.* Beta-galactosidase histochemistry and telomere loss in senescent retinal pigment epithelial cells. *Investigative ophthalmology & visual science* **40**, 197–202 (1999).

21. Lee, B. Y. *et al.* Senescence-associated β-galactosidase is lysosomal β-galactosidase. *Aging cell* **5**, 187–195 (2006).

22. Severino, J., Allen, R., Balin, S., Balin, A. & Cristofalo, V. J. Is β-galactosidase staining a marker of senescence in vitro and in vivo? *Experimental cell research* **257**, 162–171 (2000).

23. Okamura-Oho, Y. *et al.* Maturation and degradation of β-galactosidase in the post-Golgi compartment are regulated by cathepsin B and a non-cysteine protease. *FEBS letters* **419**, 231–234 (1997).

24. Valieva, Y., Ivanova, E., Fayzullin, A., Kurkov, A. & Igrunkova, A. Senescence-Associated β-Galactosidase Detection in Pathology. *Diagnostics* **12**, 2309 (2022).

25. Bridger, J. M., Foeger, N., Kill, I. R. & Herrmann, H. The nuclear lamina: both a structural framework and a platform for genome organization. *The FEBS journal* **274**, 1354–1361 (2007).

26. Dechat, T. *et al.* Nuclear lamins: major factors in the structural organization and function of the nucleus and chromatin. *Genes & development* **22**, 832–853 (2008).

27. Krohne, G. & Benavente, R. The nuclear lamins: a multigene family of proteins in evolution and differentiation. *Experimental cell research* **162**, 1–10 (1986).

28. Gerace, L. & Blobel, G. The nuclear envelope lamina is reversibly depolymerized during mitosis. *Cell* **19**, 277–287 (1980).

29. Goldman, R. D., Gruenbaum, Y., Moir, R. D., Shumaker, D. K. & Spann, T. P. Nuclear lamins: building blocks of nuclear architecture. *Genes & development* **16**, 533–547 (2002).

30. Lin, F. & Worman, H. J. Structural organization of the human gene encoding nuclear lamin A and nuclear lamin C. *Journal of Biological Chemistry* **268**, 16321–16326 (1993).

31. Harborth, J., Elbashir, S. M., Bechert, K., Tuschl, T. & Weber, K. Identification of essential genes in cultured mammalian cells using small interfering RNAs. *Journal of cell science* **114**, 4557–4565 (2001).

32. Worman, H. J., Östlund, C. & Wang, Y. Diseases of the nuclear envelope. *Cold Spring Harbor perspectives in biology* **2**, a000760 (2010).

33. Scaffidi, P. & Misteli, T. Lamin A-dependent nuclear defects in human aging. *Science* **312**, 1059–1063 (2006).

34. Kim, Y. *et al.* Mouse B-type lamins are required for proper organogenesis but not by embryonic stem cells. *Science* **334**, 1706–1710 (2011).

35. Shimi, T. *et al.* The A-and B-type nuclear lamin networks: microdomains involved in chromatin organization and transcription. *Genes & development* **22**, 3409–3421 (2008).

36. Sun, L., Wu, J., Du, F., Chen, X. & Chen, Z. J. Cyclic GMP-AMP synthase is a cytosolic DNA sensor that activates the type I interferon pathway. *Science* **339**, 786–791 (2013).

37. Wu, J. *et al.* Cyclic GMP-AMP is an endogenous second messenger in innate immune signaling by cytosolic DNA. *Science* **339**, 826–830 (2013).

38. Ishikawa, H. & Barber, G. N. STING is an endoplasmic reticulum adaptor that facilitates innate immune signalling. *Nature* **455**, 674–678 (2008).

39. Ishikawa, H., Ma, Z. & Barber, G. N. STING regulates intracellular DNA-mediated, type I interferon-dependent innate immunity. *Nature* **461**, 788–792 (2009).

40. Fenech, M. *et al.* Molecular mechanisms of micronucleus, nucleoplasmic bridge and nuclear bud formation in mammalian and human cells. *Mutagenesis* **26**, 125–132 (2011).

41. Sun, B. *et al.* Dengue virus activates cGAS through the release of mitochondrial DNA. *Scientific reports* **7**, 3594 (2017).

42. Takahashi, A. *et al.* Downregulation of cytoplasmic DNases is implicated in cytoplasmic DNA accumulation and SASP in senescent cells. *Nature communications* **9**, 1249 (2018).

43. Muñoz-Espín, D. & Serrano, M. Cellular senescence: from physiology to pathology. *Nature reviews Molecular cell biology* **15**, 482–496 (2014).

44. Wiley, C. D. *et al.* Mitochondrial dysfunction induces senescence with a distinct secretory phenotype. *Cell metabolism* **23**, 303–314 (2016).

45. Campisi, J. Aging, cellular senescence, and cancer. *Annual review of physiology* **75**, 685–705 (2013).

46. Kuilman, T. *et al.* Oncogene-induced senescence relayed by an interleukin-dependent inflammatory network. *Cell* **133**, 1019–1031 (2008).

47. Hubackova, S., Krejcikova, K., Bartek, J. & Hodny, Z. IL1-and TGFβ-Nox4 signaling, oxidative stress and DNA damage response are shared features of replicative, oncogene-induced, and drug-induced paracrine 'bystander senescence'. *Aging (Albany NY)* **4**, 932 (2012).

48. Gillet, G. & Brun, G. Viral inhibition of apoptosis. *Trends in microbiology* **4**, 312–317 (1996).

49. Choi, Y., Bowman, J. W. & Jung, J. U. Autophagy during viral infection—a double-edged sword. *Nature reviews microbiology* **16**, 341–354 (2018).

50. Gugliesi, F. *et al.* Where do we stand after decades of studying human cytomegalovirus? *Microorganisms* **8**, 685 (2020).

51. Ramanan, P. & Razonable, R. R. Cytomegalovirus infections in solid organ transplantation: a review. *Infection & chemotherapy* **45**, 260 (2013).

52. Annaloro, C. *et al.* Viral infections in HSCT: detection, monitoring, clinical management, and immunologic implications. *Frontiers in immunology* **11**, 569381 (2021).

53. Cannon, M. J., Grosse, S. D. & Fowler, K. B. The epidemiology and public health impact of congenital cytomegalovirus infection. *Cytomegaloviruses: from molecular pathogenesis to intervention* **2**, 26–48 (2013).

54. Cannon, M. J., Schmid, D. S. & Hyde, T. B. Review of cytomegalovirus seroprevalence and demographic characteristics associated with infection. *Reviews in medical virology* **20**, 202–213 (2010).

55. Plosa, E. J., Esbenshade, J. C., Fuller, M. P. & Weitkamp, J.-H. Cytomegalovirus infection. *Pediatrics in review* **33**, 156–163 (2012).

56. Griffiths, P., Baraniak, I. & Reeves, M. The pathogenesis of human cytomegalovirus. *The Journal of pathology* **235**, 288–297 (2015).

57. Boppana, S. B. & Britt, W. J. Synopsis of clinical aspects of human cytomegalovirus disease. *Cytomegaloviruses: from molecular pathogenesis to intervention* **2**, 1–25 (2013).

58. Stockdale, L. *et al.* Human cytomegalovirus epidemiology and relationship to tuberculosis and cardiovascular disease risk factors in a rural Ugandan cohort. *PloS one* **13**, e0192086 (2018).

59. Fowler, K. *et al.* A systematic literature review of the global seroprevalence of cytomegalovirus: possible implications for treatment, screening, and vaccine development. *BMC Public Health* **22**, 1659 (2022).

60. Jackson, J. W. & Sparer, T. There is always another way! cytomegalovirus' multifaceted dissemination schemes. *Viruses* **10**, 383 (2018).

61. Sezgin, E., An, P. & Winkler, C. A. Host genetics of cytomegalovirus pathogenesis. *Frontiers in genetics* **10**, 616 (2019).

62. Bhat, V., Joshi, A., Sarode, R. & Chavan, P. Cytomegalovirus infection in the bone marrow transplant patient. *World journal of transplantation* **5**, 287 (2015).

63. Ong, D. S., Chong, G.-L. M., Chemaly, R. F. & Cremer, O. L. Comparative clinical manifestations and immune effects of cytomegalovirus infections following distinct types of immunosuppression. *Clinical Microbiology and Infection* **28**, 1335–1344 (2022).

64. Hummel, M. & Abecassis, M. M. A model for reactivation of CMV from latency. *Journal of Clinical Virology* **25**, 123–136 (2002).

65. Prösch, S. *et al.* Stimulation of the human cytomegalovirus IE enhancer/promoter in HL-60 cells by TNFα is mediated via induction of NF-κB. *Virology* **208**, 197–206 (1995).

66. Haspot, F. *et al.* Human cytomegalovirus entry into dendritic cells occurs via a macropinocytosis-like pathway in a pH-independent and cholesterol-dependent manner. *PloS one* **7**, e34795 (2012).

67. Diosi, P., Babusceac, L., Nevinglovschi, O. & Kun-Stoicu, G. Cytomegalovirus infection associated with pregnancy. *The Lancet* **290**, 1063–1066 (1967).

68. Dworsky, M., Yow, M., Stagno, S., Pass, R. F. & Alford, C. Cytomegalovirus infection of breast milk and transmission in infancy. *Pediatrics* **72**, 295–299 (1983).

69. Hamprecht, K. *et al.* Epidemiology of transmission of cytomegalovirus from mother to preterm infant by breastfeeding. *The Lancet* **357**, 513–518 (2001).

70. Stagno, S., Reynolds, D. W., Pass, R. F. & Alford, C. A. Breast milk and the risk of cytomegalovirus infection. *New England Journal of Medicine* **302**, 1073–1076 (1980).

71. Adler, S. P. Cytomegalovirus and child day care. *New England Journal of Medicine* **321**, 1290–1296 (1989).

72. Meyers, J. D. Cytomegalovirus infection following marrow transplantation: risk, treatment, and prevention. *Birth Defects Original Article Series* **20**, 101–117 (1984).

73. Handsfield, H. H. *et al.* Cytomegalovirus infection in sex partners: evidence for sexual transmission. *Journal of Infectious Diseases* **151**, 344–348 (1985).

74. Van den Berg, A. *et al.* Recent advances in the diagnosis of active cytomegalovirus infection after organ transplantation. in vol. 22 226–228 (1990).

75. Arvin, A. *et al.* Human herpesviruses: biology, therapy, and immunoprophylaxis. (2007).

76. Farrell, H. E., Lawler, C., Oliveira, M. T., Davis-Poynter, N. & Stevenson, P. G. Alveolar macrophages are a prominent but nonessential target for murine cytomegalovirus infecting the lungs. *Journal of virology* **90**, 2756–2766 (2016).

77. Heldwein, E. E. gH/gL supercomplexes at early stages of herpesvirus entry. *Current opinion in virology* **18**, 1–8 (2016).

78. Ryckman, B. J., Jarvis, M. A., Drummond, D. D., Nelson, J. A. & Johnson, D. C. Human cytomegalovirus entry into epithelial and endothelial cells depends on genes UL128 to UL150 and occurs by endocytosis and low-pH fusion. *Journal of virology* **80**, 710–722 (2006).

79. Wang, D. & Shenk, T. Human cytomegalovirus virion protein complex required for epithelial and endothelial cell tropism. *Proceedings of the National Academy of Sciences* **102**, 18153–18158 (2005).

80. Wille, P. T., Knoche, A. J., Nelson, J. A., Jarvis, M. A. & Johnson, D. C. A human cytomegalovirus gO-null mutant fails to incorporate gH/gL into the virion envelope and is unable to enter fibroblasts and epithelial and endothelial cells. *Journal of virology* **84**, 2585–2596 (2010).

81. Wille, P. T., Wisner, T. W., Ryckman, B. & Johnson, D. C. Human cytomegalovirus (HCMV) glycoprotein gB promotes virus entry in trans acting as the viral fusion protein rather than as a receptor-binding protein. *MBio* **4**, 10–1128 (2013).

82. Sinzger, C. *et al.* Fibroblasts, epithelial cells, endothelial cells and smooth muscle cells are major targets of human cytomegalovirus infection in lung and gastrointestinal tissues. *Journal of General Virology* **76**, 741–750 (1995).

83. Poole, E. *et al.* Alveolar macrophages isolated directly from human cytomegalovirus (HCMV)–seropositive individuals are sites of HCMV reactivation in vivo. *The Journal of Infectious Diseases* **211**, 1936–1942 (2015).

84. Silva, M. C., Schröer, J. & Shenk, T. Human cytomegalovirus cell-to-cell spread in the absence of an essential assembly protein. *Proceedings of the National Academy of Sciences* **102**, 2081–2086 (2005).

85. Noriega, V. M. *et al.* Human cytomegalovirus US28 facilitates cell-to-cell viral dissemination. *Viruses* **6**, 1202–1218 (2014).

86. Pannuti, C. S. *et al.* Cytomegalovirus mononucleosis in children and adults: differences in clinical presentation. *Scandinavian journal of infectious diseases* **17**, 153–156 (1985).

87. Zanghellini, F., Boppana, S. B., Emery, V. C., Griffiths, P. D. & Pass, R. F. Asymptomatic primary cytomegalovirus infection: virologic and immunologic features. *The Journal of infectious diseases* **180**, 702–707 (1999).

88. Drew, W. L. *et al.* Frequency and duration of plasma CMV viremia in seroconverting blood donors and recipients. *Transfusion* **43**, 309–313 (2003).

89. Britt, W. Manifestations of human cytomegalovirus infection: proposed mechanisms of acute and chronic disease. *Human cytomegalovirus* 417–470 (2008).

90. Streblow, D. N., Dumortier, J., Moses, A. V., Orloff, S. L. & Nelson, J. A. Mechanisms of cytomegalovirus-accelerated vascular disease: induction of paracrine factors that promote angiogenesis and wound healing. *Human Cytomegalovirus* 397–415 (2008).

91. Boeckh, M. & Geballe, A. P. Cytomegalovirus: pathogen, paradigm, and puzzle. *The Journal of clinical investigation* **121**, 1673–1680 (2011).

92. Chan, G., Bivins-Smith, E. R., Smith, M. S. & Yurochko, A. D. Transcriptome analysis of NF-κB-and phosphatidylinositol 3-kinase-regulated genes in human cytomegalovirus-infected monocytes. *Journal of virology* **82**, 1040–1046 (2008).

93. Landolfo, S., Gariglio, M., Gribaudo, G. & Lembo, D. The human cytomegalovirus. *Pharmacology & Therapeutics* **98**, 269–297 (2003).

94. Britt, W. J. & Mach, M. Human cytomegalovirus glycoproteins. *Intervirology* **39**, 401–412 (1996).

95. Lu, M. & Shenk, T. Human cytomegalovirus UL69 protein induces cells to accumulate in G1 phase of the cell cycle. *Journal of virology* **73**, 676–683 (1999).

96. Hayashi, M. L., Blankenship, C. & Shenk, T. Human cytomegalovirus UL69 protein is required for efficient accumulation of infected cells in the G1 phase of the cell cycle. *Proceedings of the National Academy of Sciences* **97**, 2692–2696 (2000).

97. Liu, B. & Stinski, M. F. Human cytomegalovirus contains a tegument protein that enhances transcription from promoters with upstream ATF and AP-1 cis-acting elements. *Journal of virology* **66**, 4434–4444 (1992).

98. Baldick Jr, C. J., Marchini, A., Patterson, C. E. & Shenk, T. Human cytomegalovirus tegument protein pp71 (ppUL82) enhances the infectivity of viral DNA and accelerates the infectious cycle. *Journal of virology* **71**, 4400–4408 (1997).

99. Bresnahan, W. A. & Shenk, T. E. UL82 virion protein activates expression of immediate early viral genes in human cytomegalovirus-infected cells. *Proceedings of the National Academy of Sciences* **97**, 14506–14511 (2000).

100. Romanowski, M. J., Garrido-Guerrero, E. & Shenk, T. pIRS1 and pTRS1 are present in human cytomegalovirus virions. *Journal of virology* **71**, 5703–5705 (1997).

101. Shang, Z. & Li, X. Human cytomegalovirus: pathogenesis, prevention, and treatment. *Molecular Biomedicine* **5**, 61 (2024).

102. Raviola, S. *et al.* Human cytomegalovirus infection triggers a paracrine senescence loop in renal epithelial cells. *Communications Biology* **7**, 292 (2024).